Mixed-mode bursting oscillations: Dynamics created by a slow passage through spike-adding canard explosion in a square-wave burster

Mathieu Desroches, Tasso J. Kaper, and Martin Krupa

Additional information on Chaos
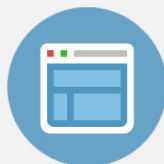
Mixed-mode bursting oscillations: Dynamics created by a slow passage through spike-adding canard explosion in a square-wave burster

Mathieu Desroches,[1] Tasso J. Kaper,[2] and Martin Krupa[1]

[1]*INRIA Paris-Rocquencourt Research Centre, MYCENAE Project-Team, Domaine de Voluceau, Rocquencourt BP 105, 78153 Le Chesnay cedex, France*
[2]*Department of Mathematics and Statistics, Center for BioDynamics, Boston University, 111 Cummington Mall, Boston, Massachusetts 02215, USA*

This article concerns the phenomenon of Mixed-Mode Bursting Oscillations (MMBOs). These are solutions of fast-slow systems of ordinary differential equations that exhibit both small-amplitude oscillations (SAOs) and bursts consisting of one or multiple large-amplitude oscillations (LAOs). The name MMBO is given in analogy to Mixed-Mode Oscillations, which consist of alternating SAOs and LAOs, without the LAOs being organized into burst events. In this article, we show how MMBOs are created naturally in systems that have a spike-adding bifurcation or spike-adding mechanism, and in which the dynamics of one (or more) of the slow variables causes the system to pass slowly through that bifurcation. Canards are central to the dynamics of MMBOs, and their role in shaping the MMBOs is two-fold: saddle-type canards are involved in the spike-adding mechanism of the underlying burster and permit one to understand the number of LAOs in each burst event, and folded-node canards arise due to the slow passage effect and control the number of SAOs. The analysis is carried out for a prototypical fourth-order system of this type, which consists of the third-order Hindmarsh-Rose system, known to have the spike-adding mechanism, and in which one of the key bifurcation parameters also varies slowly. We also include a discussion of the MMBO phenomenon for the Morris-Lecar-Terman system. Finally, we discuss the role of the MMBOs to a biological modeling of secreting neurons. © *2013 AIP Publishing LLC*. [http://dx.doi.org/10.1063/1.4827026]

This study introduces a new mechanism for generating complex oscillations in systems of differential equations with fast and slow time scales. At the heart of the model, there is a third-order system of equations, which exhibits spike-adding transitions. Then, when the bifurcation parameter that controls the spike-adding transition is allowed to evolve slowly in time, a new mechanism for generating oscillations arises. The resulting solutions possess alternating segments of small-amplitude slow oscillations (SAOs) and bursts, which consist of large-amplitude fast oscillations (LAOs). Hence, the solutions are termed Mixed-Mode Bursting Oscillations (MMBOs), in analogy with the known Mixed-Mode-Oscillations (MMO) that consist of alternating SAOs and LAOs without the LAOs being organized in bursts. Moreover, MMBOs may be periodic or aperiodic. The large-amplitude oscillations in the bursts are created by the slow passage through the spike-adding bifurcation, and the number of small-amplitude oscillations is controlled by the system parameters and by the presence of a certain type of singularity in the slow subsystem. While the results are presented for the Hindmarsh-Rose (H-R) model, they apply to a broad class of fast-slow neuronal oscillators, including the Morris-Lecar-Terman model and others that exhibit the spike-adding transition. The analysis also raises timely mathematical questions related to understanding the new dynamics created by combining bursting and MMO dynamics.

I. INTRODUCTION

MMOs is a term used to describe trajectories that combine small-amplitude oscillations and large-amplitude oscillations of relaxation type, both recurring in an alternating manner. Recently, there has been a lot of interest in MMOs that arise due to a generalized canard phenomenon.[4,7,15,20,22] Such MMOs arise in the context of slow-fast systems with at least two slow variables and with a folded critical manifold (set of equilibria of the fast system). The small oscillations arise during the passage of the trajectories near a fold, due to the presence of a so-called *folded singularity*. The dynamics near the folded singularity is transient, yet recurrent: the trajectories return to the neighborhood of the folded singularity by way of a global return mechanism.

An important step on the way to an understanding of MMOs is the analysis of the flow near the folded singularities. Of particular importance are special solutions called *canards*. The term canard was first used to denote periodic solutions of the van der Pol equation that stay close to the repelling slow manifold (which lies close to the middle branch of the fast nullcline).[1] One of the characteristic features of canard cycles is that they exist only for an exponentially small range of parameter values. This very sharp transition was then termed *canard explosion*.[3] The related term canard solution has been used to denote solutions connecting an attracting slow manifold to a repelling slow manifold. Such canards, sometimes also called *maximal canards*, organize the dynamics in a similar way as invariant sets

which separate different dynamical regimes (e.g., separatrices of saddle points). Also, in systems with more than one slow variable, canards occur in a more robust fashion and underlie the presence of the small-amplitude oscillations near the folded singularity in MMOs.

When going from two to three dimensions in slow-fast vector fields, one may add a second fast variable instead of a second slow variable. In that case, the fast dynamics can now sustain periodic dynamics and this can give rise, in the full three-dimensional system, to complex oscillations referred to as *bursting oscillations*. Such systems are then called *bursters*. Bursters have long been studied using a slow-fast dynamics formalism and then classified by a number of different means, including the bifurcations of the fast system in which the burst events are initiated and terminated[16,27] and by an unfolding theory approach to singularities in the fast subsystem.[11] Among the many known bursters is the one giving rise to so-called *square-wave bursting*, where the burst phase is initiated by a saddle-node bifurcation of equilibria and ends in a homoclinic bifurcation. It is a "two fast/one slow" system for which the critical manifold (fast nullcline) is a cubic curve. The H-R system[13,14] is one of the simplest square-wave bursters since it corresponds to a (smooth) polynomial vector field (Eqs. (1)–(3) below). In this model, bursting solutions arise through a supercritical Hopf bifurcation followed by a canard explosion; then a canard-mediated spike-adding transition is responsible for bursting orbits with more and more fast oscillations in the burst. This phenomenon is well-known and has been investigated, for instance, in the Morris-Lecar-Terman model[12,33] and in the Hindmarsh-Rose model;[24,25,34] see Sec. III.

An open question involves what happens when a system exhibits slow passage through the spike-adding bifurcation, and it is this question which we address in this article. We show that slow passage through a spike-adding bifurcation gives rise to complex oscillations. The solutions exhibit complex oscillations with small-amplitude oscillations around the fold point of the fast nullcline, interspersed with large-amplitude oscillations, but contrary to MMOs, the large-amplitude oscillations occur in bursts. This is why we choose

to name this more elaborate type of complex oscillations *Mixed-Mode Bursting Oscillations* or *MMBOs*. A principal difference here is that the system has two fast variables, which allows for fast oscillations; then, the fast component of the periodic attractors are the bursts. See Fig. 1.

MMBOs are also relevant in the modeling of biological rhythms. For instance, the model of pancreatic β-cells proposed by Bertram *et al.* in Ref. 2 has the right structure to sustain MMBOs and the time series shown in Ref. 2 (e.g., Fig. 3) clearly displays both small-amplitude slow oscillations and bursts of large-amplitude fast oscillations.

In this article, we investigate the presence of MMBOs in the following system:

$$x' = y - ax^3 + bx^2 + I - z, \tag{1}$$

$$y' = c - dx^2 - y, \tag{2}$$

$$z' = \varepsilon(s(x - x_1) - z), \tag{3}$$

$$I' = \varepsilon(k - h_x(x - x_{\text{fold}})^2 - h_y(y - y_{\text{fold}})^2 - h_I(I - I_{\text{fold}})). \tag{4}$$

System (1)–(4) is an extension of the H-R burster, where the main bifurcation parameter, the applied current I, evolves slowly. In Eq. (4), the I component of the vector field is an elementary model for dynamical clamping of the current, in that it accounts for the lowest order terms that would be present in a generic dynamical clamping protocol that slowly adjusts the applied current. In Eqs. (1)–(3), which correspond to the H-R system, we consider the classical parameter values, as follows: $a = 1$, $b = 3$, $c = 1$, $d = 5$, $\varepsilon = 0.001$, $s = 4$, $x_1 = -1.618$; note that the small parameter ε is usually denoted by r. The critical manifold of the H-R burster is the curve

$$
\begin{aligned}
S_0 &= \{x' = 0\} \cap \{y' = 0\} \\
&= \{z = -ax^3 + (b - d)x^2 + I + c\}.
\end{aligned} \tag{5}
$$

The terms x_{fold} and y_{fold} correspond to the lower fold point of S_0. Therefore, we have
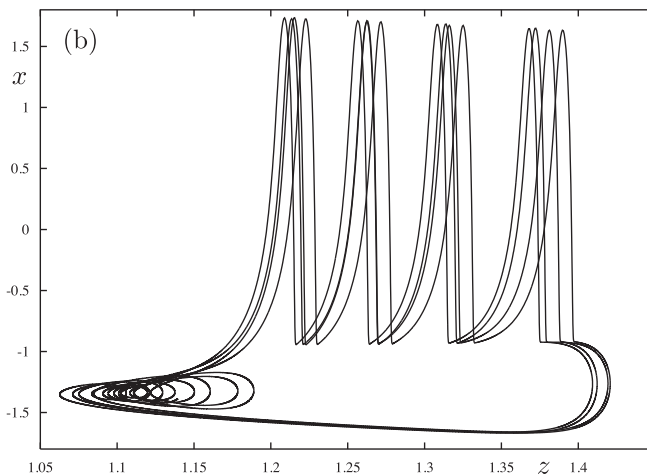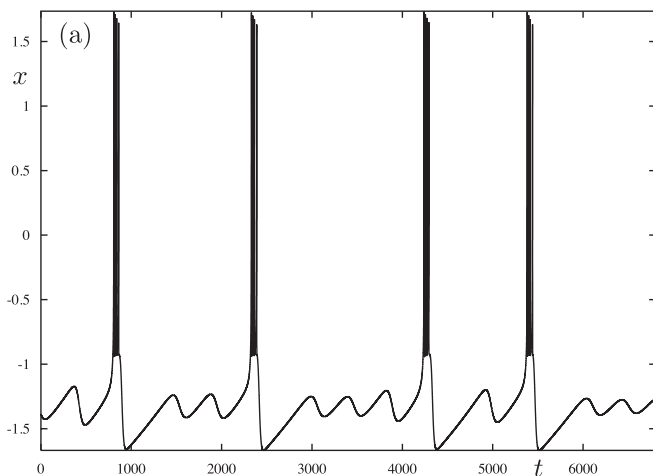

FIG. 1. Simulation of system (1)–(4) for $\varepsilon = 10^{-3}$, $k = 10^{-2}$, and $h_i = 10^{-2}$ for $i = x, y, I$. The orbit shown here is clearly of MMBO type, that is, a succession of small-amplitude slow oscillations and large-amplitude fast oscillations. The observed MMBO pattern is irregular and combines transitions of the type 4^1, 4^2, and 4^3.
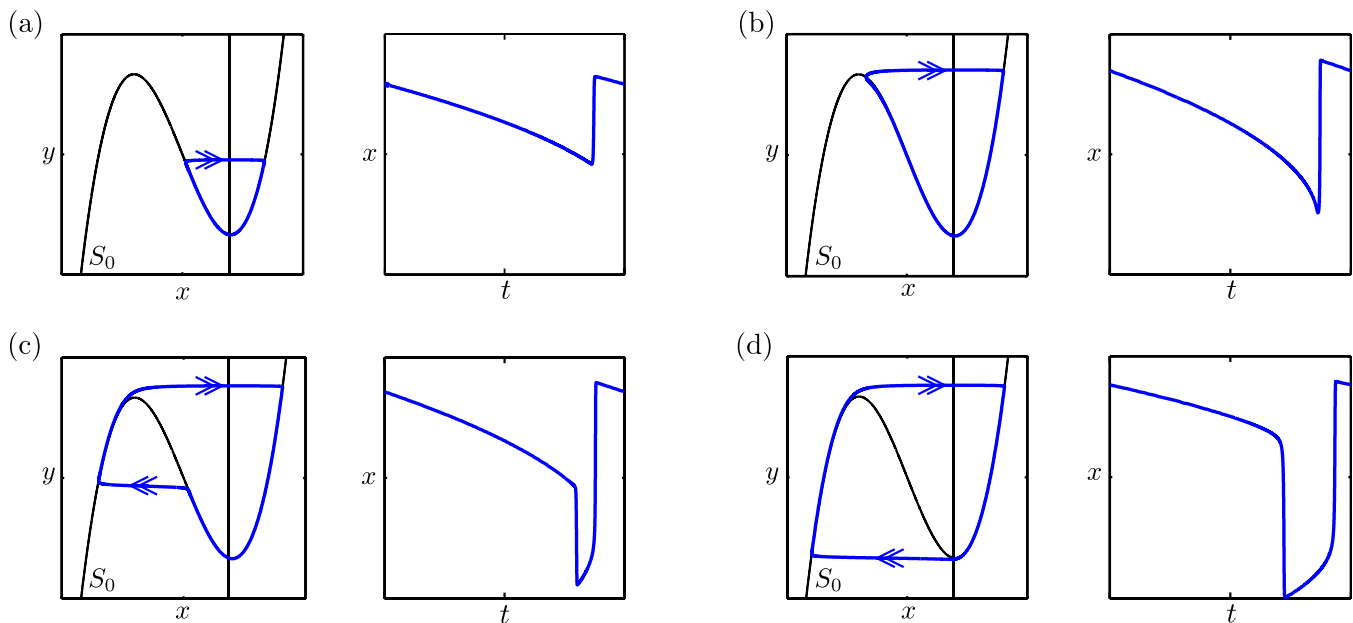
FIG. 2. Canard explosion at the lower fold in the van der Pol system: the slow and the fast dynamics must be as shown and the slow nullcline (shown in black), must cross the fold transversely. Four cycles are presented (in blue): headless canard in panel (a), maximal canard in panel (b), canard with head in panel (c), and relaxation oscillation in panel (d). In each panel, the left plot corresponds to a phase plane representation of the cycle together with the fast cubic nullcline S_0 and the slow linear nullcline (both in black); the right panel shows the time series of the x variable during the cycle.

$$x_{\text{fold}} = \frac{2(b-d)}{3a}, \quad y_{\text{fold}} = c - dx_{\text{fold}}^2. \quad (6)$$

Furthermore, the value I_{fold} is chosen so that the slow nullcline of the H-R burster $\{z = s(x - x_1)\}$ goes exactly through the fold of S_0. Thus, we have

$$I_{\text{fold}} = ax_{\text{fold}}^3 - (b-d)x_{\text{fold}}^2 + s(x_{\text{fold}} - x_1) - c. \quad (7)$$

The main new result is that slow passage through I_{fold} combined with a suitable return mechanism leads to MMBOs. More generally, our goals in this article are to understand the dynamics of MMBOs, in particular, to show that they result from a slow passage through a spike-adding canard explosion and to show how the number of SAOs is controlled, via folded node theory, by the system parameter k. Along the way, we will show in this article that the point $(I_{\text{fold}}, 0)$ in the parameter space (I, ε) is the accumulation point of the wedges corresponding to spike adding transitions. We add that the transition we study results in a system that has a folded node singularity with a global return that includes bursting dynamics of square wave type and which maps the trajectories leaving the folded node region back to the funnel region of the folded node. This description is a generalization of the characterization of the MMO dynamics given in Ref. 4.

The results of this article may be generalized to other problems where a spike-adding transition occurs. The principal requirement is that the parameter which unfolds this transition evolves slowly in the full system.

The H-R model has been used as a simple framework for single-cell dynamics, in relation to neurological diseases such as epilepsy.[26] We extend the H-R model by putting a slow dynamics on the applied current I. Kispersky et al.[28] created a biophysically accurate model of a stellate cell from

the entorhinal cortex and argued that the STO dynamics occurring in this model could be linked to the presence of hyperexcitability in models of temporal lobe epilepsy.[21] This mechanism relies on strong sensitivity of the neuronal model to parameter variation, which is a property of the dynamics considered in this paper. We provide a canonical description of a very sensitive parameter region where small variation of a parameter could lead to large changes of dynamics and in particular of the firing rate. Moreover, the use of a phenomenological model (as opposed to a biophysical model) provides a theoretical/canonical framework to analyze dynamic properties of MMBOs observed in both healthy and diseased neurons in a way that is independent of the details of the participating ionic currents that are responsible for each aspect of the dynamics.

The article is organized as follows. In Sec. II, we review the canard explosion phenomenon in classical planar fast-slow systems. In Sec. III, we examine the phenomenon of spike-adding via canards in the third-order vector-field (1)–(3), with I as a parameter. Then, in Sec. IV, we present the dynamics of Eqs. (1)–(4), and the appearance of orbits formed by a slow passage through a spike-adding transition: these are MMBOs; we then state the main characteristics of MMBOs. The article ends with a discussion in Sec. V.

II. BRIEF REVIEW OF CLASSICAL CANARD EXPLOSION

In this section, we briefly review the classical limit cycle canards and the canard explosion in planar slow-fast systems

$$x' = f(x, y), \quad (8)$$

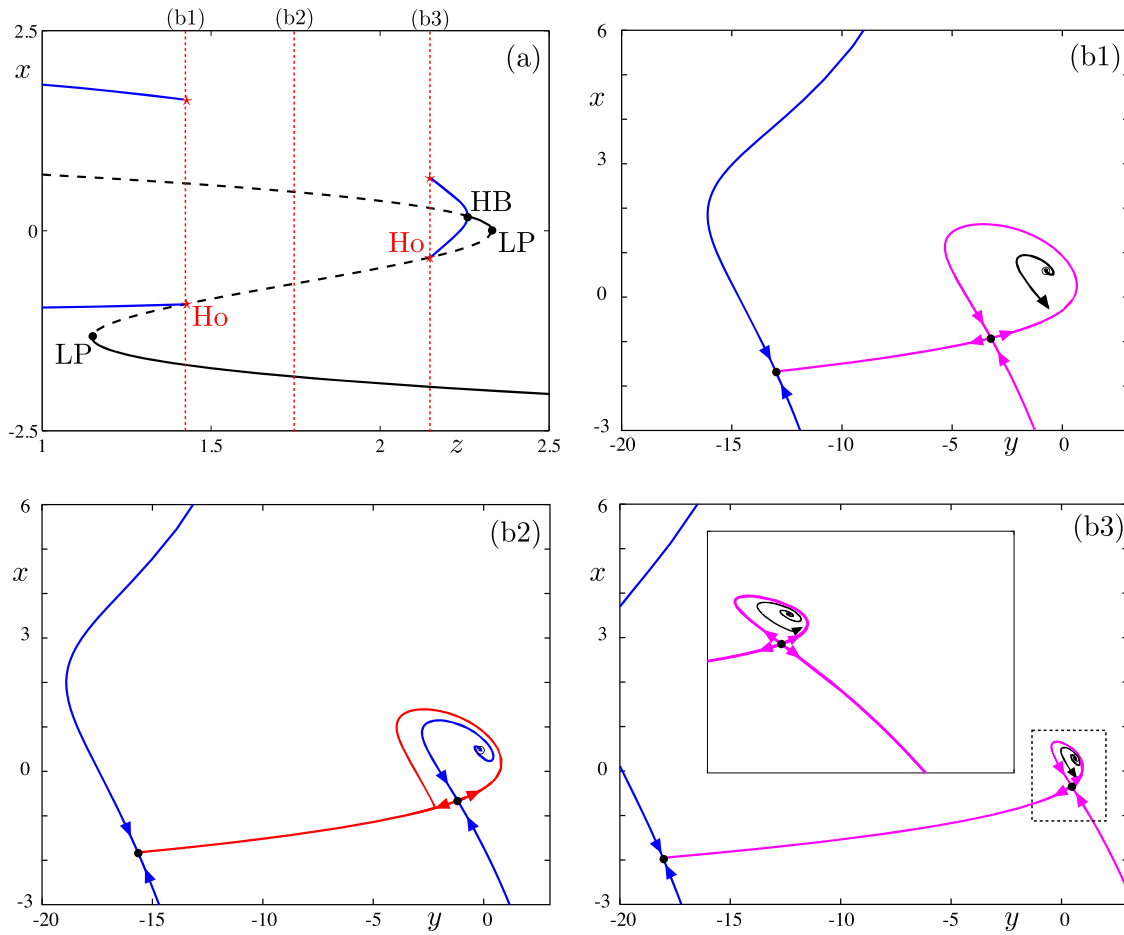$$y' = \varepsilon g(x, y, \lambda). \quad (9)$$

FIG. 3. Panel (a) shows the bifurcation diagram of the fast subsystem of the Hindmarsh-Rose burster, i.e., Eqs. (1) and (2), with z acting as a parameter. All parameter values are taken to be the classical ones (Sec. I) and I is fixed at the value corresponding to the canard explosion taking place in the full system and displayed in Fig. 4, that is, $I = 1.3278138$. Panels (b1)-(b3) show snapshots of the phase portrait of the fast system for three different values of z, namely, $z = 1.449$ (lower homoclinic), $z = 1.75$ and $z = 2.180$ (upper homoclinic). For each value of z in between the lower and upper homoclinics, the unstable manifold of the saddle returns to a neighbourhood of the saddle and gives the leading-order location of the spike in the full system.

Here, $0 < \varepsilon \ll 1$ is the small parameter measuring the separation of time scales, and $\lambda \in \mathbb{R}$ is a parameter.

For $\varepsilon = 0$, these systems have a critical manifold (the fast nullcline) $S_0 = \{f(x, y) = 0\}$. This manifold is often an S-shaped curve with two non-degenerate quadratic fold points (x_m, y_m) and (x_M, y_M), where $f(x_i, y_i) = 0$ and $\partial f/\partial x(x_i, y_i) = 0$ for $i = m, M$. In addition, we assume that for a locally unique value, λ_0, of the parameter λ, $g(x_m, y_m, \lambda_0) = 0$ and $\frac{\partial g}{\partial \lambda}(x_m, y_m, \lambda_0) \neq 0$. Hence, the slow nullcline transversely intersects S_0 at one of the fold points, here the local minimum (x_m, y_m), and the slow nullcline passes through this fold point with non-zero speed as λ changes through λ_0.

Under these conditions, system (8) and (9) exhibits a standard canard explosion.[1,3,9,10,18] We illustrate this for the van der Pol equation in Fig. 2, with $f(x, y) = y - (x^3/3 - x)$ and $g(x, y, \lambda) = \lambda - x$. There is a Hopf bifurcation when the slow nullcline crosses any of the fold points of S_0, that is, at $\lambda = \lambda_H = \pm 1$. In Fig. 2(a), a limit cycle canard known as a headless duck is shown. It has long segments near the attracting slow manifold (near the right branch of S_0) and the repelling slow manifold (near the middle branch of S_0) in alternation and a fast jump from the latter back to the former

to complete the cycle. Fig. 2(b) illustrates the maximal headless canard, which occurs for the unique parameter value, $\lambda_c = \lambda_0 - (1/8)\varepsilon - (3/32)\varepsilon^2 + O(\varepsilon^3)$, at which the attracting and repelling slow manifolds coincide. Then, for λ on the other side of λ_c, the limit cycle canard jumps from the repelling (middle) branch to the left attracting slow manifold, forming a duck with a head, as shown in Fig. 2(c). Finally, for values of λ at the extreme of the canard explosion interval, the periodic solution is a full-blown relaxation oscillation, see Fig. 2(d).

We observe that even a standard canard explosion in slow-fast systems with one slow variable and one fast variable need not always be monotonic in the regular parameter (λ in the context of this section), see, e.g., Ref. 18. In other words, for some systems, the sequence of parameter values of λ corresponding to the canards in the canard explosion is a non-monotone sequence, within the exponentially small interval. A very simple example of this is, for some parameter values, the FitzHugh-Nagumo system. This feature may result in the presence of turning points as well the coexistence of canard cycles for the same value of λ, but it does not alter the fundamental features of canard explosion, like the closeness to singular cycles and the exponentially narrow
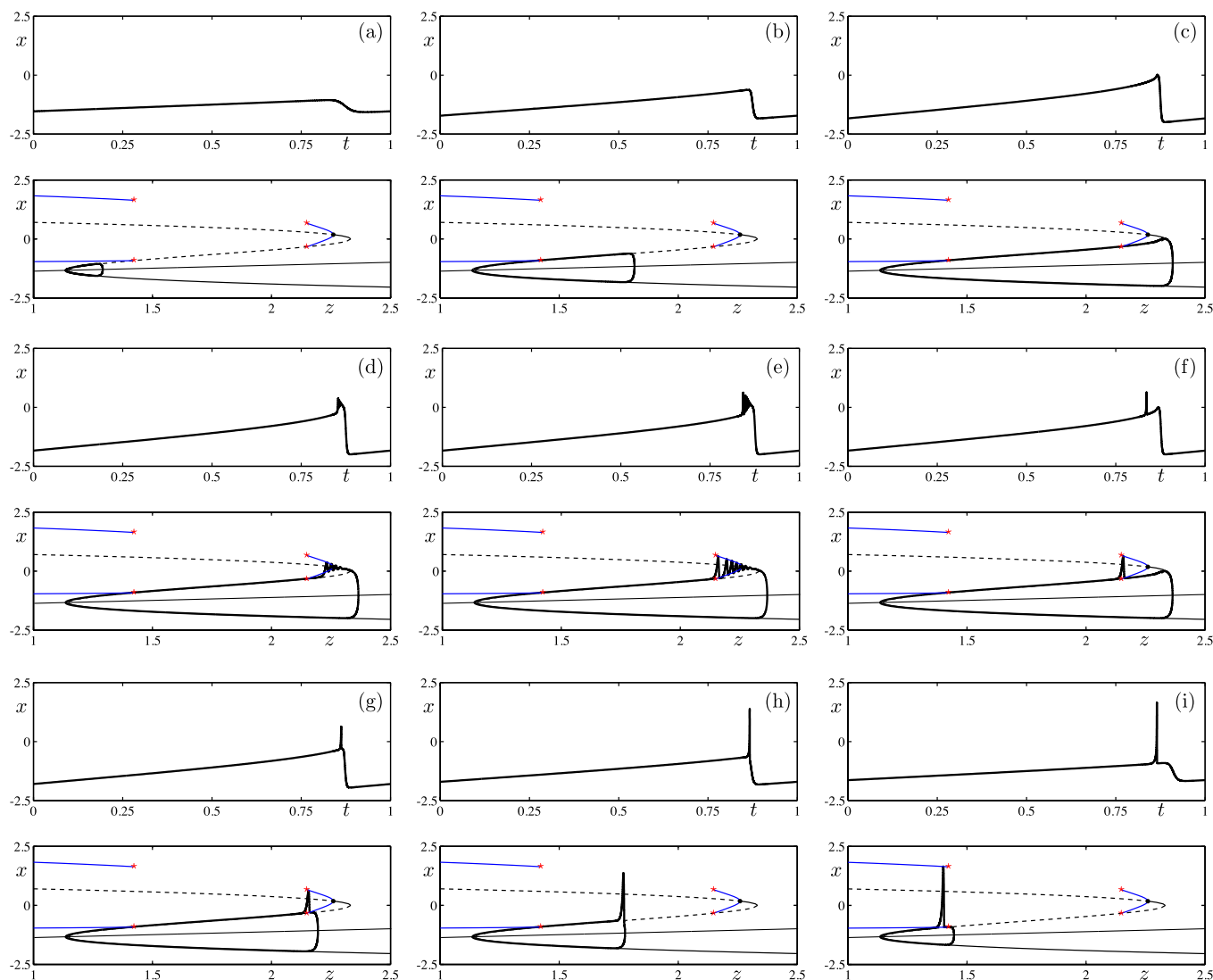
FIG. 4. Spike-adding phenomenon: time series and phase portraits for the sequence of limit cycle canards observed in the transition from 0 to 1 spike in the Hindmarsh-Rose system (1)–(3). Parameter values are those given below Eqs. (1)–(3), with $\varepsilon = 5 \times 10^{-4}$ and I varying by an exponentially small amount around the value of 1.3278138026. The top plot in each panel (a) to (i) shows the time series of the x-variable, with the period normalised to 1. The bottom plot shows the limit cycle canard in the phase plane (x, z). In each frame, the behaviour of the trajectory at the end of the canard segment can be understood by looking at the phase portrait of the fast system (1) and (2) shown in Fig. 3.

width of the parameter interval. Due to this complication, one usually does not think of a branch of canard cycles as parametrized by λ but rather as a curve parametrized by λ and another quantity characterizing the solution, which could be amplitude, often used in the context of Hopf bifurcations, L_2 norm, the height of the corresponding singular canard,[18] etc. The choice often made in the case of canards, partly imposed by the continuation program AUTO,[8] is to use L_2 norm. Keeping in mind this non-monotonicity, we will describe the evolution of canard solutions referring as a function of their position on the branch rather the corresponding value of the parameter, which does not need to be unique.

III. SPIKE-ADDING CANARD EXPLOSION IN THE HINDMARSH-ROSE SYSTEM

In this section, we examine the transition from a stable equilibrium (quiescence) to stable square-wave bursting in the Hindmarsh-Rose system (1)–(3) for a sequence of fixed

values of the parameter I. This sequence is centered about the value of I corresponding to the value of the canard explosion in the full system, and a sequence of phase portraits of the fast system (1)–(2) for this value of I is shown in Figure 3, for some representative values of z. This transition occurs via the well-known mechanism of spike-adding, see Refs. 12, 24, 25, and 34, first analyzed in the Morris-Lecar-Terman model, see Ref. 33. For each $N = 0, 1, 2\ldots$, there is an exponentially narrow interval of parameter values I over which the system exhibits a continuous transition from periodic solutions with N spikes to periodic solutions with $N + 1$ spikes. Each periodic solution in the transition sequence is referred to as a canard of limit cycle type, or limit cycle canard, since each periodic orbit has alternating segments near attracting and repelling branches of fixed points interspersed with fast jumps from the latter to the former that reinitiate the cycle. Each transition sequence is referred to as a canard explosion, and the transitions for $N = 0$ and $N = 1$ are illustrated in Figs. 4 and 5, respectively.
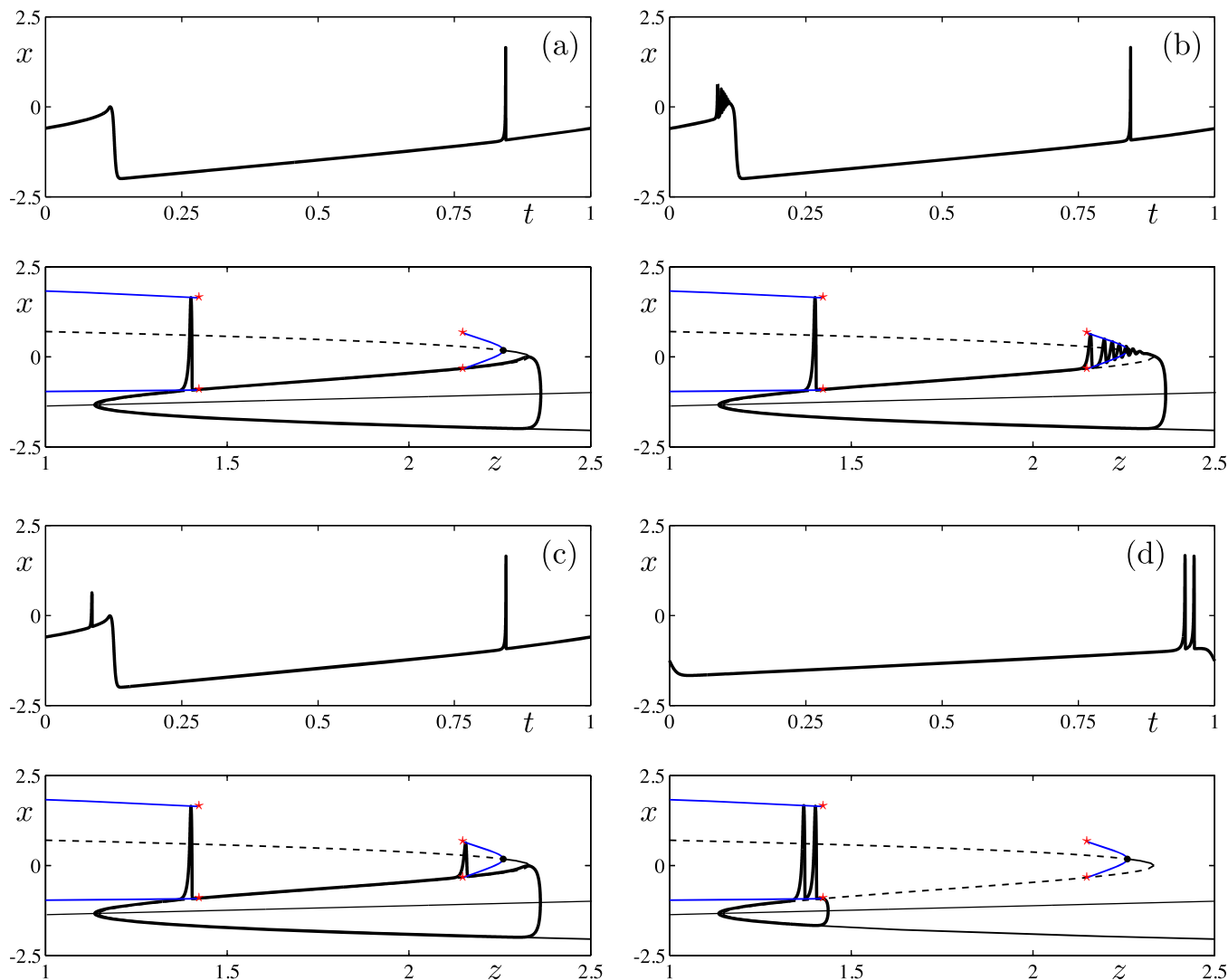
FIG. 5. Spike-adding phenomenon: time series and phase plane projections for limit cycles along the transition from 1 spike to 2 spikes. The first spike, created during the previous spike-adding transition, remains in essentially the same place during the transition in which the second spike is generated. Along the explosion that leads to the addition of a second spike, the parameter I varies by an exponentially amount around the value of 1.3317831217.

A detailed description of the transition for $N=0$ from quiescence to a limit cycle with one large-amplitude spike is as follows. At $I \approx 1.413$, there is a Hopf bifurcation of the full system (1)–(3). This Hopf bifurcation induces the canard explosion, in exact analogy to that in the planar van der Pol and FitzHugh-Nagumo equations. For $I = 1.3278138093$, the H-R system (1)–(3) exhibits a small-amplitude limit cycle canard without any spike, also known as a headless canard, see Fig. 4(a). As I is decreased, see Fig. 4(b), the limit cycle grows in amplitude until, at $I = 1.3278138026$, it reaches the far right fold near $z = 2.328$, see Fig. 4(c). This is the maximal headless canard, and as in the canonical planar systems with canards, such as the van der Pol and FitzHugh-Nagumo equations, it occurs precisely when the persistent attracting and repelling slow manifolds near the branches of equilibria coincide. Although slow manifolds are in general not unique, there are unique analytic slow manifolds near the attracting branches of the critical manifold.[35] Besides, one can choose a repelling slow manifold that starts $O(\sqrt{\varepsilon})$ near the canard point and continues to $O(\varepsilon^{1/3})$ close to the jump point following the repelling branch; the power of ε is dictated by the

choice of the blow-up transformation needed to analyse the underlying singularity: canard point or fold point. Therefore, one can study the intersection between the attracting and the repelling slow manifolds; see Ref. 19 for details.

Further along the branch, the limit cycle continues to have long segments near both the attracting and the repelling branches of the critical manifold, but now at the end of the segment near the repelling branch there is a brief segment of small oscillations, see Figs. 4(d) and 4(e), since the orbit now jumps from the critical manifold up to the branch of attracting periodic orbits, instead of back down to the branch of the critical manifold corresponding to attracting fixed points of the fast system. The attracting slow manifold now lies above the repelling slow manifold so that solutions must jump up to the branch of attracting periodic orbits. Even further along the branch, the up-jump occurs near the homoclinic orbit near $z = 2.180$, and the oscillations disappear, see Fig. 4(f). There is a long segment near the branch of repelling fixed points again, so that the canard cycles in this range have two canard segments, with the spike in between them.

The second canard segment disappears as we move yet further along the branch, see Fig. 4(g). Then, toward the end of the canard explosion, the location of the spike shifts downward in z, see Fig. 5(h), until the spike occurs near the lower homoclinic ($z = 1.449$). This completes the description of how the first large-amplitude spike is created in a continuous manner as the parameter I is changed, so that continuous dependence of solutions on parameters is respected, and it completes the description of the first cycle of spike-adding, for $N = 0$.

The continuous transition for $N = 1$, from a limit cycle canard with one spike to a limit cycle canard with two spikes, occurs in a completely analogous fashion, see Fig. 5. During this second canard explosion, the first spike remains near $z = 1.449$. The sequence in which the second spike is created is precisely the same as that in which the first spike was created in Fig. 4 above. Moreover, we refer to this as the knitting mechanism. One creates loops in knitting in a similar manner, by hooking the yarn over the tip of the needle (here the far right fold point) and then pulling it back along the needle.

It is worth observing also that, not only are the intervals of parameter values I in which each of these canard explosions for $N = 0, 1, 2, \ldots$ occur exponentially small in the limit as $\varepsilon \to 0$, but the critical values of I, at which the maximal headless ducks with N spikes occur, also approach each other as $\varepsilon \to 0$. Hence, the entire sequence of canard explosions occurs in an exponentially small interval of I values.

The dynamics of the canard limit cycles during each of these canard explosions is richer than that observed in planar systems such as the van der Pol and the FitzHugh-Nagumo equations because the repelling slow manifold is of saddle type here with two-dimensional stable and unstable manifolds. Indeed, according to the position of the orbit with respect to these manifolds, it will either follow the slow manifold along a canard segment or escape from it along a fast fiber; see Ref. 12 for details. The transition can be understood by invoking the *Exchange Lemma*.[17]

For parameter values of I when the spike is first created, see Figs. 4(f) and 5(c), the spike lies close to the (upper) homoclinic of the fast system. Then, further along the branch, the limit cycle canard still exhibits a spike, however there is no homoclinic orbit of the fast system nearby, see Fig. 3(b2). Nevertheless, in the full third-order system, the one-dimensional repelling slow manifold has two-dimensional stable and unstable manifolds whose relative positions are responsible for the creation of the spike. These positions are given to leading order by the stable and unstable manifolds of the saddle repelling fixed point in the fast system, as shown in Fig. 3(b2).

Finally, to give further perspective on these results, we describe the classical square wave burster, as analyzed by Terman.[33] In general position, such a solution behaves as a relaxation oscillator near the lower fold and jumps to an attracting manifold corresponding to fast oscillations. Subsequently, the solution follows the manifold of stable fast oscillations until it terminates near the homoclinic orbit of the fast system, whereupon the solution jumps down to the stable branch of the slow manifold. As explained in

Ref. 33, the number of fast oscillations is unbounded as $\varepsilon \to 0$. Although we are sure that this is folklore information, we have not found an asymptotic estimate of the number of such oscillations. We have derived such an estimate and included it in this paper in Appendix. Our calculation implies that the number of such oscillations is $O(1/\varepsilon)$. It follows that changes of I by $O(\varepsilon)$ may result in spike adding transitions of the same kind as the latter part of our spike adding canard explosion as well as the spike adding transitions described by Terman[33] or Guckenheimer and Kuehn.[12] Such spike adding transitions do not contain classical canard cycles but they contain canard segments corresponding to passage near the middle part of the critical manifold (see Figure 3(b) of Ref. 33) and they occur in exponentially small intervals of I. As pointed out by Terman[33] and further elaborated on by Guckenheimer and Kuehn,[12] such transitions do not have to be monotonic in I and may lead to chaotic dynamics. Due to the computational complexity (a large number of spikes), we do not show an AUTO plot of such a transition.

IV. MMBOs AS A SLOW PASSAGE THROUGH A SPIKE-ADDING CANARD EXPLOSION

In this section, we study the full system (1)–(4), in which I is also a slow variable. We show that the full system exhibits a broad class of new solutions known as MMBOs, which are periodic or aperiodic solutions that consist of two distinct phases: a segment of SAOs in alternation with a burst event or multiple burst events, with each burst comprising one or more LAOs or spikes. A prototypical MMBO of the full system has been presented in Fig. 1. There, a variable number of SAOs (ranging from one to three) occur in alternation with a burst event that consists of four LAOs.

In Sec. IV A, we study the MMBOs in the slow passage through canard explosion regime. We show that the LAOs occur due to slow passage through the spike-adding bifurcation, coupled with a global return mechanism. In this regime, for moderate values of ε, the MMBO patterns found are quite complicated and can evolve dynamically in time. In contrast, in Sec. IV B, we use the theory of folded nodes for fast-slow systems to show that the number of SAOs in a MMBO may be controlled by the system parameter k. The observed MMBO patterns are then much more regular and correspond to smaller values of ε. The notation for a MMBO with s SAOs and ℓ LAOs per burst is ℓ^s. With this notation, MMOs are simple examples of MMBOs.

A. Understanding MMBOs as a slow passage through a canard explosion

In this section, we focus on the dynamics of MMBO trajectories as a slow passage through a canard explosion. Hence, in this section, we consider the case of ε relatively large.

The MMBOs are characterized by the number of SAO during the first phase and the number of bursts during the second phase, as well as the number of LAOs within each burst. An elementary example is given by the MMBO shown in Fig. 6(a). It consists of one SAO followed by a single burst event, which consists of eight LAOs, and this pattern repeats
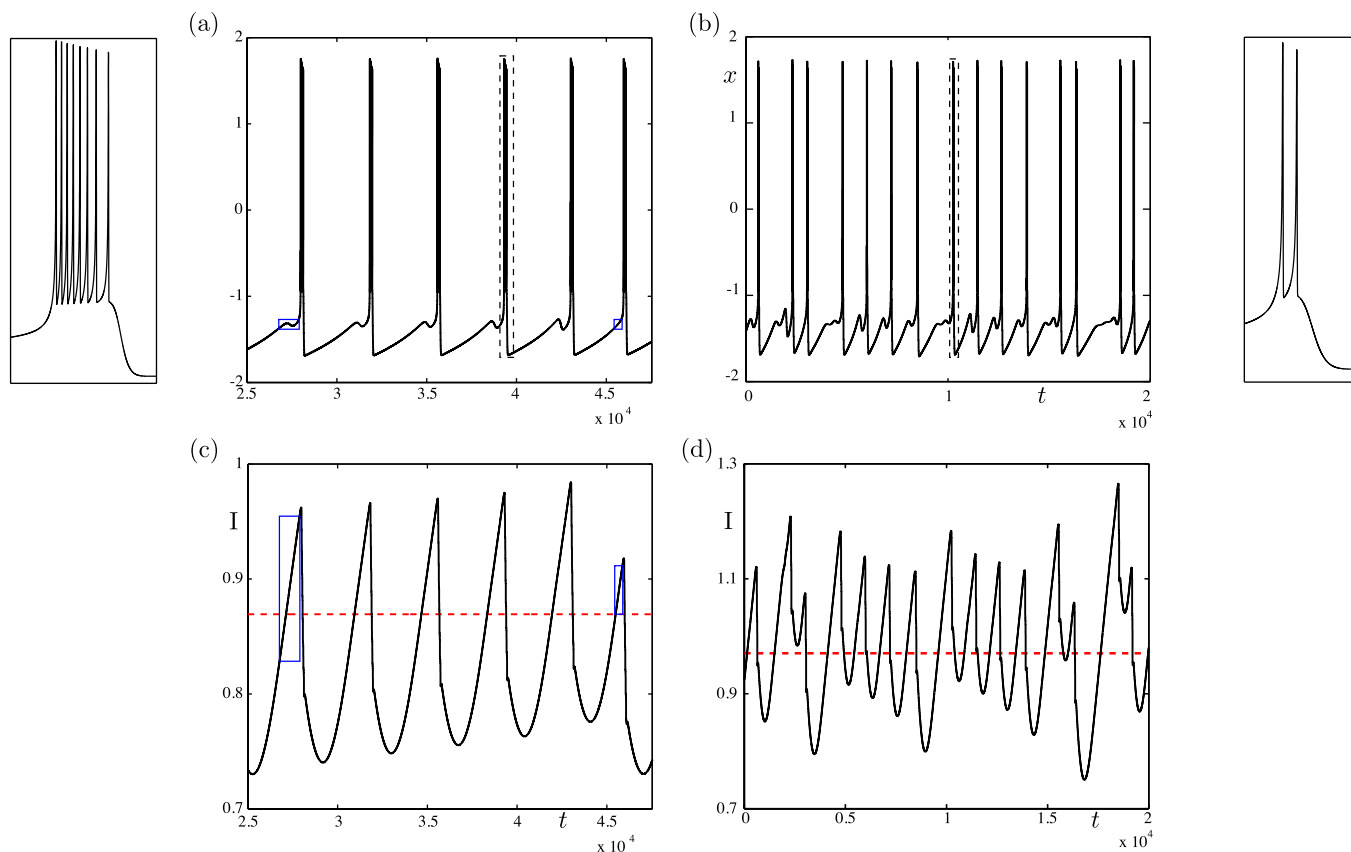
FIG. 6. Periodic MMBOs of system (1)–(4), for $k = 0.45, \varepsilon = 2.5 \cdot 10^{-4}$ (panel (a) for the x variable and panel (c) for the I variable) and $k = 0.35, \varepsilon = 10^{-3}$ (panels (b) and (d) for the x variable and the I variable, respectively); in all panels, $h_x = 5$ and $h_y = h_I = 10^{-2}$. In panels (c) and (d), the dashed red curve indicates the value of I corresponding to the folded node. The unlabelled panels to the side of panel (a) and panel (b) show zooms into one burst of the corresponding MMBO, with 8 LAOs (left panel) and 2 LAOs (right panel).

five times. Then, after the fifth transition of this type, there is a burst with seven LAOs, which is not preceded by a SAO. Overall, this $8^1 8^1 8^1 8^1 8^1 7^0$ repeats itself for time up to at least $t = 100\,000$, and only a segment of amplitude about $20\,000$ is shown.

Within the cycle of the five successive 8^1, the SAO have increasing amplitudes. The time series for the variable I shown in Fig. 6 reveals that the I variable repeatedly passes through the interval (centered about $I = 0.869$) corresponding to the spike-adding mechanism; this value corresponds to the I-value of the folded node, we indicate it as a dashed red curve in both panels (c) and (d) for each value of k. With each passage, the value of z at which the jump from the branch of repelling equilibria up to the branch of attracting periodic orbits occurs decreases slightly, so that the resulting SAO has a larger amplitude.

Next, the fact that after the fifth 8^1 there is no SAO preceding the LAOs may be understood as follows. From the plots of the x and I variables, one sees that if the orbit reaches the fold of S_0 after I goes above the value of the folded node then it does not complete a SAO but directly jumps to the LAO regime; see the blue boxes in Figs. 6(a) and 6(c). Hence, there is no SAO preceding the subsequent LAOs. Also, within the sequence of 8^1, the amplitudes of the successive SAOs increase, marking a dynamic approach to the first secondary canard.

Finally, the fact that after the fifth 8^1 the following burst has lost one LAO can be understood by looking at the time

evolution of I; see Fig. 6(c). Indeed, the loss of the SAO due to the slow passage through a canard explosion induces the orbit to jump at the lower fold and start the burst earlier. The dynamics of I is affected and as a result it changes the location of the homoclinic connection of the fast subsystem, whose associated saddle equilibrium happens for a lower value of z. This explains why the burst is shorter in this case.

Another prototypical MMBO is shown in Fig. 6(b), but now the pattern is highly irregular. We see alternations between the basic blocks 2^2, 2^0 and 2^1. Focusing on the LAOs which are not preceded by SAOs, three of which occur in the time series shown, one near the beginning and two near the end, we see from the times series of the I-variable that the value of I does not dip below I_{fold}, which explains the absence of SAOs. One may use a similar explanation by looking at the behaviour of the I-variable during the three corresponding peaks.

What we have just seen with the two examples of MMBOs shown in Fig. 6 is valid for "moderate" values of ε, that is, such that ε does not become very small relative to k. In this situation, the slow passage through canard explosion can modify dynamically the number of SAOs within one transition, and the I dynamics can also alter the number of LAOs within each burst due to changes in the location of the homoclinic connection in the underlying fast subsystem. However, in order to understand the MMBO pattern using folded node theory, one has to decrease ε substantially.
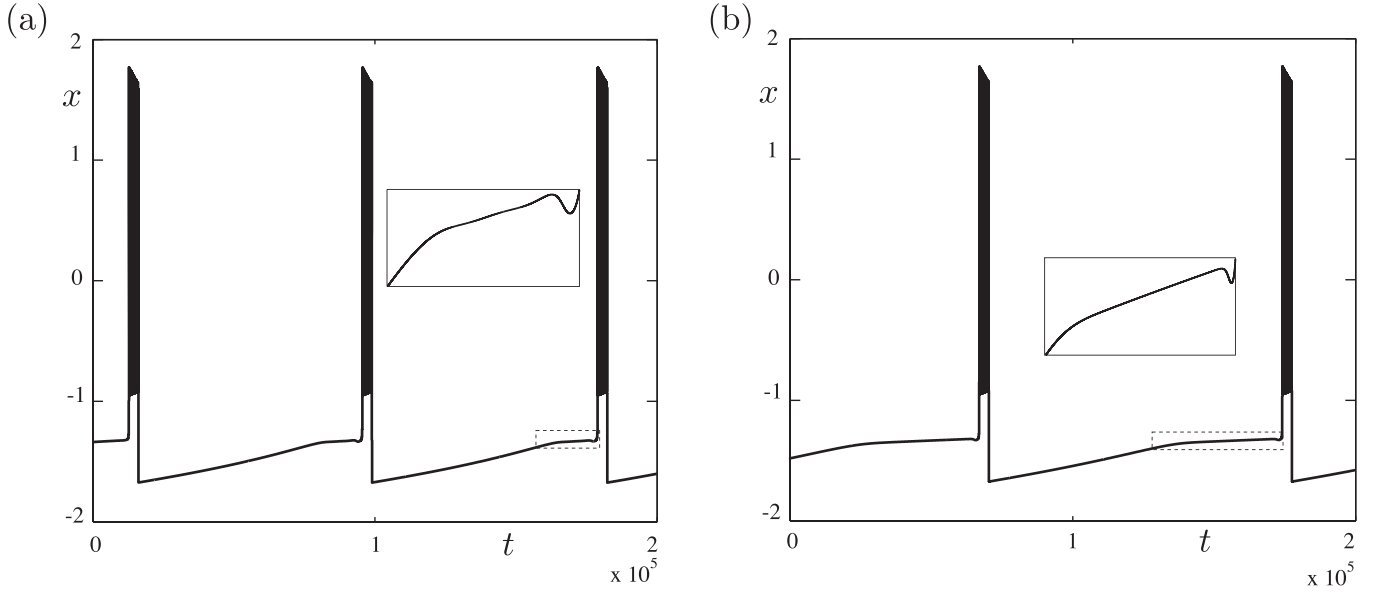
(a)

(b)

FIG. 7. Periodic MMBOs of system (1)–(4), for $k = 0.45$ (panel (a)) and $k = 0.35$ (panel (b)) and for $\varepsilon = 10^{-5}$; in both panels $h_x = 5$ and $h_y = h_I = 10^{-2}$. Decreasing ε allows to find MMBOs with the correct number of SAOs as predicted by folded node theory via formula (16). In both cases, the number of LAOs is very large, about 200.

The patterns gain more LAOs per burst and become more regular as the parameter ε is decreased. The MMBOs shown in Figs. 7(a) and 7(b) are for the same parameter values as those shown in Figs. 6(a) and 6(b), however the values of ε are much smaller. In particular, while one sees the pattern $8^1 8^1 8^1 8^1 8^1 7^0$ for $k = 0.45$ and $\varepsilon = 0.001$ in Fig. 6(a), one sees a periodic N^3 pattern with $N = 192$ for the much smaller value $\varepsilon = 10^{-5}$, as shown in Fig. 7(a). Similarly, with $k = 0.35$, the pattern becomes a regular N^5 pattern with $N = 194$ for $\varepsilon = 10^{-5}$, as shown in Fig. 7(b). The number of spikes per burst has increased dramatically because of the chasm between the fast and slow timescales when $\varepsilon = 10^{-5}$. Moreover, as we will show in Subsection IV B, the number of SAOs has increased from 3 to 5 as k is decreased, due to the dynamics near the folded node.

B. Controlling the number of SAOs in MMBOs using folded node theory

In Sec. IV A, we have discussed a series of transitions which occur upon variation of I and lead to MMBO dynamics. As a result one obtains a system with a folded node point and a global return passing through bursting dynamics. This is a generalization of the perspective on MMOs given in Ref. 4; consequently a prototypical context of MMBOs is a combination of folded node dynamics with a global return including bursting dynamics and returning the trajectories which leave the folded node region back to the funnel of the folded node, see also Ref. 2. In this section, we consider the case when $I < I_{\text{fold}}$ (sufficiently close to I_{fold}). In this case, there is a folded node in the four-dimensional extended Hindmarsh-Rose system (1)–(4). We determine the number of SAOs in a given MMBO by using the local folded node theory from Ref. 31 and its extension to systems with two fast dimensions.[4]

Changing to the slow time $\tau = \varepsilon t$ gives the equivalent system

$$
\begin{aligned}
\varepsilon \dot{x} &= y - ax^3 + bx^2 + I - z, \\
\varepsilon \dot{y} &= c - dx^2 - y, \\
\dot{z} &= s(x - x_1) - z, \\
\dot{I} &= k - h_x(x - x_{\text{fold}})^2 - h_y(y - y_{\text{fold}})^2 - h_I(I - I_{\text{fold}}).
\end{aligned}
\tag{10}
$$

The $\varepsilon = 0$ limit of system (10) gives the singular approximation to the slow dynamics or *reduced system*, that is, differential equations for the slow variables z and I constrained by algebraic equations defining the fast nullsurface, that is, the critical manifold S_0, recall (5). This manifold is a cubic hypersurface in $\mathbb{R}^4$. By projection onto the three-dimensional phase space (x, z, I), S_0 is a cubic surface with two curves of fold points (with respect to the fast variable x) F^+ and F^-, given by

$$
F^+ = \{x = 0\}, \quad F^- = \left\{ x = \frac{2(b - d)}{3a} \right\}.
$$

Differentiating the algebraic condition (5) defining S_0 with respect to time gives a differential equation for x

$$
\begin{aligned}
x(3ax - 2(b - d))\dot{x} &= \dot{I} - \dot{z} \\
&= -ax^3 + (b - d)x^2 + I + c - s(x - x_1) \\
&\quad + k - h_x(x - x_{\text{fold}})^2 - h_y(y - y_{\text{fold}})^2 \\
&\quad - h_I(I - I_{\text{fold}}).
\end{aligned}
$$

It is customary to append to that equation one slow equation, for instance that of I. The resulting two-dimensional system is singular along the fold set $F = F^+ \cup F^-$ of S_0. In order to

extend that system up to the fold set F, one typically desingularises it by performing a time rescaling, here with a factor $x(3ax - 2(b - d))$; see, for instance, Refs. 4 and 32 for the general theory. Therefore, one obtains a planar non-singular system given by

$$\dot{x} = -ax^3 + (b - d)x^2 + I + c - s(x - x_1) + k$$
$$- h_x(x - x_{\text{fold}})^2 - h_y(y - y_{\text{fold}})^2 - h_I(I - I_{\text{fold}}), \quad (11)$$

$$\dot{I} = x(3ax - 2(b - d))(k - h_x(x - x_{\text{fold}})^2 - h_y(y - y_{\text{fold}})^2$$
$$- h_I(I - I_{\text{fold}})). \quad (12)$$

System (11) and (12) is called the *Desingularised Reduced System (DRS)*. Equilibria of the DRS lying on F are called *pseudo-equilibria* or *folded singularities* for the original system given that they are not equilibrium solutions there. We focus on the folded singularity satisfying $x_{\text{f}} \neq 0$, that is,

$$x_{\text{f}} = \frac{2(b - d)}{3a} = x_{\text{fold}}. \quad (13)$$

From the previous equality comes immediately that $y_{\text{f}} = y_{\text{fold}}$. Using the x-equation of the DRS, we find that

$$I_{\text{f}} = \frac{ax_{\text{fold}}^3 - (b - d)x_{\text{fold}}^2 - c + s(x_{\text{fold}} - x_1) - k - h_I I_{\text{fold}}}{1 - h_I}.$$

In the first four terms of the numerator above, we recognise the expression of I_{fold} given in (7). Therefore, we have

$$I_{\text{f}} = I_{\text{fold}} - \frac{k}{1 - h_I}. \quad (14)$$

Now, the Jacobian matrix of the DRS at the folded singularity $(x_{\text{f}}, I_{\text{f}})$ is given by

$$\begin{pmatrix} -s & 1 - h_I \\ (6ax_{\text{f}} - 2(b - d))(k - h_I(I_{\text{f}} - I_{\text{fold}})) & 0 \end{pmatrix}.$$

Using Eqs. (13) and (14), we see that the lower left entry further simplifies to

$$2(b - d)\frac{k}{1 - h_I}.$$

Consequently, the two eigenvalues of the folded singularity are given by

$$\lambda_{\pm} = 0.5\left(-s \pm \sqrt{s^2 + 8k(b - d)}\right),$$

which gives a node provided that $s^2 + 8k(b - d) > 0$ and $b - d < 0$. Finally, we obtain the following expression for the eigenvalue ratio μ at the folded node

$$\mu = \frac{\lambda_+}{\lambda_-} = \frac{s\left(s - \sqrt{s^2 + 8k(b - d)}\right) + 4k(b - d)}{4k(d - b)}. \quad (15)$$

This ratio μ determines n, the number of SAOs, as follows. The general theory, see, for instance, Ref. 4, states that for

$0 < \varepsilon \ll 1$ small enough, there are at most $n + 1$ small oscillations near the folded node, that is, n secondary canards and $n + 1$ sectors of rotation, where

$$2n + 1 < \frac{1}{\mu} < 2n + 3 \quad (n \in \mathbb{N}).$$

In the present case, for the fixed (classical) parameter values $s = 4$, $b = 3$, and $d = 5$, formula (15) reduces to

$$\mu = \frac{2(1 - \sqrt{1 - k}) - k}{k}. \quad (16)$$

In Fig. 7, we show a periodic MMBO pattern 1_3^{192} obtained by direct simulation for $k = 0.45$, that is, $1/\mu \approx 6.74$, and $\varepsilon = 10^{-5}$. Therefore, based on Eq. (16), one expects at most three small oscillations and three sectors of rotation, separated by the strong canard γ_s and two secondary canards. We show both the time profile of that solution as well as its projection onto the (x, y, z)-space. Reducing ε allows one to observe the correct number of SAOs around the folded node p_{f} of the system, as predicted by theory; see Ref. 4. Indeed, in Fig. 7(a), we find 3 SAOs, as predicted by formula (16). Similarly, for $k = 0.35$, the theory predicts $1/\mu \approx 9.32$, that is, 5 SAOs and that is exactly what is shown in Fig. 7(b), which shows the MMBO pattern of 194^5.

The number of SAOs will typically be constant and maximal only for MMBOs which are not close to spike adding in their burst segment. As a MMBO undergoes a spike adding transition the return point on the stable slow manifold can move quite wildly, passing between different sectors of rotation. This can result in the presence of very complicated patterns, not just in the part of the burst segment of the dynamics but also in the segment corresponding to SAOs.

C. Slow manifolds and sectors of rotation

We present in Fig. 8 the trajectory shown in Fig. 7(a) projected onto the (x, z, I)-space and plotted together the critical manifold S_0, the lower fold curve F^- as well as the folded node p_{f}. Near the folded node of system (1)–(4), the flow is essentially three-dimensional and the dynamics is organised by the two-dimensional slow manifolds that exist in this region of phase space. The attracting and repelling slow manifolds can intersect transversely along trajectories: these are the secondary canards; see Ref. 4 for details.

We computed slow manifolds near the folded node of system (1)–(4) for parameter values that correspond to the MMBO Γ shown in Figs. 7 and 8, using a computational strategy developed in Ref. 6, namely, the numerical continuation of orbit segment solution of boundary-value problems. The result is presented in Fig. 9 where we show the computation of an attracting slow manifold S_ε^a as well as the associated maximal canards for the chosen parameter values (corresponding to the MMBO Γ): the strong canard γ_S as well as two secondary canards. They form a partition of S_ε^a into three sectors of rotations, which we named s_i, $i = 1, 2, 3$. It is clear from that figure that the periodic MMBO Γ returns in the maximal sector s_3, which justifies that it has the maximal number of small oscillations. The return of trajectories
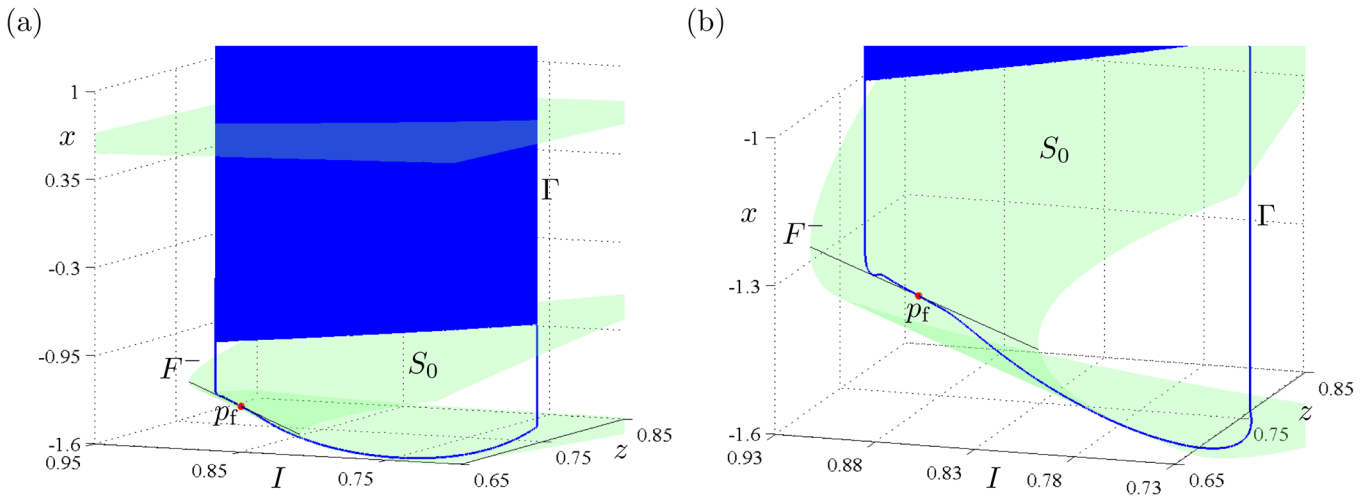
(a)

(b)

FIG. 8. Periodic 192^3-MMBOs of system (1)–(4), obtained for $k = 0.45$, that is, $1/\mu \approx 6.74$, and $\varepsilon = 10^{-5}$, and projected onto the (x, z, I)-space; also shown are the critical manifold S_0 and the lower fold curve F^-. Panel (b) is an enlargement of panel (a) near the folded node $p_f = (x_f, y_f, z_f, I_f)$.

is organised by the dynamics of I and thus it depends on the parameter k and h_i, $i = x, y, I$. For a fixed value of k, that is a fixed value of μ, we can vary any of the parameters h_i (using numerical continuation) and we can compute the distance δ between the point where the associated trajectories return on S_ε^a and the strong canard γ_s. As δ increases, all the sectors can be visited by the corresponding trajectories; see Refs. 7 and 20 for more details on the effect of δ. This parameter δ behaves linearly as a function of h_i, $i = x, y, I$ (data not shown).

V. DISCUSSION AND FUTURE WORK

In this article, we presented the new phenomenon of MMBOs in 4D slow-fast systems with two slow variables and two fast variables. MMBOs are solutions with both small-amplitude slow oscillations and large-amplitude fast oscillations organised in bursts. We constructed a minimal
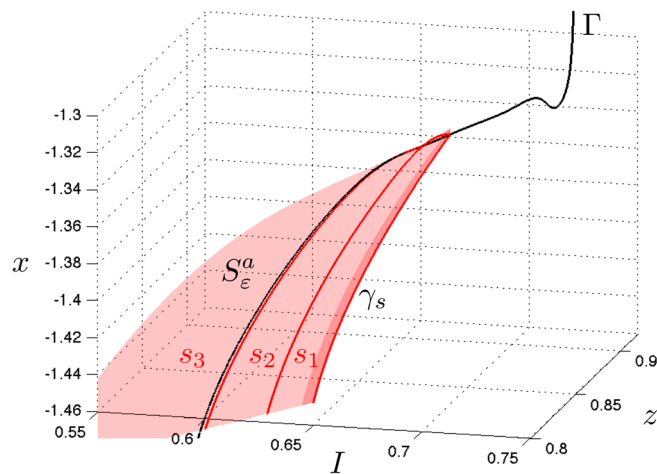

FIG. 9. Periodic 1^2-MMBOs Γ of system (1)–(4), obtained for $k = 0.45$, that is, $1/\mu \approx 6.74$, and $\varepsilon = 10^{-5}$, and projected onto the (x, z, I)-space; also shown are a numerical computation of an attracting slow manifold S_ε^a. We highlight three orbits on S_ε^a: the strong canard γ_s as well as two (unlabelled) secondary canards; these define three rotation sectors named s_i, $i = 1, 2, 3$. The number of SAO in a given solution depends on which sector it lies in; in particular, in sector s_i solutions have i SAOs.

system, based on the Hindmarsh-Rose burster, displaying MMBOs by considering an extension of the Hindmarsh-Rose burster in the spike-adding regime. The MMBOs were all created as a result of slow passage the through spike-adding transition. There is a folded node in the full system (1)–(4), and we verified that, for ε sufficiently small, the number of SAOs in MMBO trajectories follows the formula predicted by folded node theory. Moreover, we showed that the LAOs in MMBO trajectories are generated by the slow passage through the spike-adding transition.

The parameter region of MMBOs is defined by the presence of a folded node as well as bursting dynamics. At the boundary of the MMBO parameter region, one can access different dynamical regimes: MMOs without bursting, bursting without SAOs, spiking, and quiescence. More specifically, if the return to the stable branch is not into the funnel region then SAOs will disappear and the observed behavior will be that of classical bursting. Moving in another parameter direction, e.g., towards the folded saddle-node transition, will result in the number of SAOs tending to infinity, thus, making the quiescent phase longer. Eventually, spiking will cease. Finally, an important transition in bursters is when bursting solutions give way to spiking solutions; one can expect that, in some parameter direction, one can lose the burst, replaced by isolated LAOs, then the full solution will become a MMO in the usual sense.

The analysis presented in this article holds for any system with two slow and two fast variables with a folded node or a folded saddle-node of type II[7,20] and with a fast dynamics qualitatively similar to the Hindmarsh-Rose model. In particular, the current results are of interest for other bursters, including the Morris-Lecar-Terman model.[12,33] The Morris-Lecar-Terman system is known to display spike-adding transitions. Furthermore, the bifurcation structure of the fast system is slightly simpler due to the absence of Hopf bifurcation on the upper branch of the critical manifold. Therefore, it is to be expected that by allowing the corresponding parameter to evolve slowly, one will create MMBO dynamics in the resulting extended system.

Note that we chose to construct MMBOs starting from a burster and adding a second slow variable, hence creating a slow passage, and therefore, the possibility for SAOs; however, one could as well construct MMBOs, by starting from a folded node type system with two slow and one fast dimensions and suitably adding a fast dimension. In this paper, we focused on the first "route" to MMBO dynamics as we thought it was the most natural; finding an example of the second one is an interesting topic for future work.

The MMBO dynamics is relevant for other neuronal models. We were initially inspired by the time series from a model of pancreatic β-cells by Bertram et al.,[2] see Figure 3. MMBO dynamics should also be relevant for models of secreting neurons, in particular GnRH neurons.[5]

As mentioned in the introduction, the H-R model has been used as a phenomenological description of neurons in the context of epilepsy.[26] The generalised H-R model studied in this work supports a variety of dynamical regimes, including MMBOs. Different dynamical behaviours can be reached by small variation of parameters and can correspond to both healthy and pathological neuronal activity. Future work should include addressing questions about the dynamics of these neurons embedded in networks with different types of architectures, for instance in the small-world network architecture, which has been used to study epilepsy.[23]

It is interesting to note that elliptic bursting oscillations could be seen as a type of generalized MMBOs. Elliptic bursting time series are certainly visually similar to that of MMBOs; however, they appear to be different in nature since their SAOs correspond to fast oscillations, rather than oscillations on a slow or intermediate time scale. This contrasts with the time series of the MMBOs studied in this article, which are a combination of the time series of canard-mediated MMOs and of bursters.

Finally, there are a number of mathematical questions that this work has generated. For instance, proving rigorously the persistence of periodic orbits in the extended system where the main parameter organising the spike-adding transition evolves slowly. These questions are the subject of current investigation.

ACKNOWLEDGMENTS

APPENDIX: ASYMPTOTICS OF THE NUMBER OF SPIKES PER BURST AS $\varepsilon \to 0$

Given a system of the form

$$x' = f(x,y)$$
$$y' = \varepsilon g(x,y), \quad x \in \mathbb{R}^2, \quad y \in \mathbb{R}. \tag{A1}$$

Suppose that for $\varepsilon = 0$ there exists a family of periodic orbits of the layer problem $x' = f(x,y)$, parametrized monotonically by y, continuing from a Hopf bifurcation to a

homoclinic orbit. We denote the periodic orbits in this family by $p(t, y)$, with T_y denoting the period of the orbit $t \to p(t,y)$. The set

$$M_0 = \cup\{p(t,y) : t \in [0, T_y), \quad y \in (y_{\text{Hopf}}, y_{\text{hom}})\},$$

is a normally hyperbolic attracting invariant manifold M_0 for $\varepsilon = 0$ (excluding the immediate neighborhood of the Hopf bifurcation). Since it is normally hyperbolic, it persists to a nearby invariant manifold M_ε. The evolution of y for the vector field restricted to M_ε, is given by

$$y' = \varepsilon g(p(t,y),y) + O(\varepsilon^2).$$

Discarding the $O(\varepsilon)$ and averaging, we obtain

$$y' = \varepsilon \frac{1}{T_y} G(y),$$

where

$$G(y) = \int_0^{T_y} g(p(\tau,y),y)d\tau,$$

see, for example, Ref. 29 or Ref. 30. To find the lowest order approximation to the number of rotations incurred as the flow passes from $y = 0$ to $y = y_{\text{hom}}$, we note that the increment in the amount of rotation incurred as y moves from some y_0 to $y_0 + \Delta y$ is given by

$$\Delta R = \frac{\Delta t}{T_{y_0}} = \frac{1}{\varepsilon} \frac{\Delta y}{G(y_0)}.$$

Hence,

$$R = \frac{1}{\varepsilon} \int_{y_{\text{Hopf}}}^{y_{\text{hom}}} \frac{dy}{G(y)}.$$

Finally, if a trajectory of Eq. (A1) is attracted to M_ε close to a periodic orbit corresponding to some y_0 between y_{Hopf} and y_{hom}, then the estimate of the number of fast oscillations it makes is given by

$$R(y_0) = \frac{1}{\varepsilon} \int_{y_0}^{y_{\text{hom}}} \frac{dy}{G(y)}.$$

[1] E. Benoît, J.-L. Callot, F. Diener, and M. Diener, "Chasse au canard," Collect. Math. **32**, 37–119 (1981).
[2] R. Bertram, J. Rhoads, and W. P. Cimbora, "A phantom bursting mechanism for episodic bursting," Bull. Math. Biol. **70**(7), 1979–1993 (2008).
[3] M. Brøns, "Bifurcations and instabilities in the Greitzer model for compressor system surge," Math. Eng. Ind. **2**(1), 51–63 (1988).
[4] M. Brøns, M. Krupa, and M. Wechselberger, "Mixed-mode oscillations due to the generalized canard mechanism," Fields Inst. Commun. **49**, 39–63 (2006).
[5] F. Clément and J.-P. Françoise, "Mathematical modeling of the GnRH pulse and surge generator," SIAM J. Appl. Dyn. Syst. **6**(2), 441–456 (2007).
[6] M. Desroches, B. Krauskopf, and H. M. Osinga, "The geometry of slow manifolds near a folded node," SIAM J. Appl. Dyn. Syst. **7**(4), 1131–1162 (2008).
[7] M. Desroches, J. Guckenheimer, B. Krauskopf, C. Kuehn, H. M. Osinga and M. Wechselberger, "Mixed-mode oscillations with multiple time scales," SIAM Rev. **54**(2), 211–288 (2012).

[8]E. J. Doedel, R. C. Paffenroth, A. R. Champneys, T. F. Fairgrieve, Y. A. Kuznetsov, B. E. Oldeman, and X. J. Wang, AUTO-07P: Continuation and bifurcation software for ordinary differential equations, 2007, available for download from http://indy.cs.concordia.ca/auto.

[9]F. Dumortier and R. Roussarie, "Canard cycles and center manifolds," Mem. Am. Math. Soc. **121**(577) (1996, published online).

[10]W. Eckhaus, "Relaxation oscillations including a standard chase on French ducks," in *Asymptotic Analysis II—Surveys and New Trends*, Lecture Notes in Mathematics, Vol. 985, edited by F. Verhulst (Springer, 1983), pp. 449–494.

[11]M. Golubitsky, K. Josic, and T. J. Kaper, "An unfolding theory approach to bursting in fast-slow systems," *in Global Analysis of Dynamical Systems: Festschrift Dedicated to Floris Takens on the Occasion of his 60th Birthday*, H. W. Broer, B. Krauskopf, and G. Vegter (Institute of Physics Publication, 2001), pp. 277–308.

[12]J. Guckenheimer and C. Kuehn, "Computing slow manifolds of saddle type," SIAM J. Appl. Dyn. Syst. **8**(3), 854–879 (2009).

[13]J. L. Hindmarsh and R. M. Rose, "A model of the nerve impulse using two first-order differential equations," Nature **296**, 162–164 (1982).

[14]J. L. Hindmarsh and R. M. Rose, "A model of neuronal bursting using three coupled first order differential equations," Proc. R. Soc., London, Ser. B **221**(1222), 87–102 (1984).

[15]J. Jalics, M. Krupa, and H. G. Rotstein, "Mixed-mode oscillations in a three time-scale system of ODEs motivated by a neuronal model," Dyn. Syst. **25**(4), 445–482 (2010).

[16]E. M. Izhikevich, "Neural excitability, spiking and bursting," Int. J. Bifurcation Chaos **10**(6), 1171–1266 (2000).

[17]T. J. Kaper and C. K. R. T. Jones, "A primer on the exchange lemma for fast-slow systems," in *Multiple-Time-Scale Dynamical Systems* (Springer, New York, 2001), pp. 65–87.

[18]M. Krupa and P. Szmolyan, "Relaxation oscillation and canard explosion," J. Differ. Equations **174**(2), 312–368 (2001).

[19]M. Krupa and P. Szmolyan, "Extending geometric singular perturbation theory to nonhyperbolic points-fold and canard points in two dimensions," SIAM J. Math. Anal. **33**(1), 286–314 (2001).

[20]M. Krupa, N. Popović, N. Kopell, and H. G. Rotstein, "Mixed- mode oscillations in a three time-scale model for the dopaminergic neurons," Chaos **18**(1), 015106 (2008).

[21]S. S. Kumar and P. S. Buckmaster, "Hyperexcitability, interneurons, and loss of GABAergic synapses in entorhinal cortex in a model of temporal lobe epilepsy," J. neurosci. **26**(17), 4613–4623 (2006).

[22]A. Milik, P. Szmolyan, H. Loeffelmann, and E. Groeller, "Geometry of mixed-mode oscillations in the 3D autocatalator," Int. J. Bifurcation Chaos **8**, 505–519 (1998).

[23]T. I. Netoff, R. Clewley, S. Arno, T. Keck, and J. A. White, "Epilepsy in small-world networks," J. Neurosci. **24**(37), 8075–8083 (2004).

[24]J. Nowacki, H. M. Osinga, and K. Tsaneva-Atanasova, "Dynamical systems analysis of spike-adding mechanisms in transient bursts," J. Math. Neurosci. **2**, 7 (2012).

[25]H. M. Osinga and K. Tsaneva-Atanasova, "Dynamics of plateau bursting depending on the location of its equilibrium," J. Neuroendocrinol. **22**(12), 1301–1314 (2010).

[26]B. Percha, R. Dzakpasu, M. Żochowski, and J. Parent, "Transition from local to global phase synchrony in small world neural network and its possible implications for epilepsy," Phys. Rev. E **72**(3), 031909 (2005).

[27]J. Rinzel, "A formal classification of bursting mechanisms in excitable systems," in *Proceedings of the International Congress of Mathematicians* (1986), Vol. 1, pp. 1578–1593.

[28]T. Kispersky, J. A. White, and H. G. Rotstein, "The mechanism of abrupt transition between theta and hyper-excitable spiking activity in medial entorhinal cortex layer II stellate cells," PloS one **5**(11), e13697 (2010).

[29]J. E. Rubin and D. Terman, "Geometric singular perturbation analysis of neuronal dynamics," in *Handbook of Dynamical Systems* (Elsevier, 2002), Vol. 2, pp. 93–146.

[30]A. Shilnikov and M. Kolomiets, "Methods of the qualitative theory for the Hindmarsh-Rose model: A case study - A tutorial," Int. J. Bifurcation Chaos **18**(08), 2141–2168 (2008).

[31]P. Szmolyan and M. Wechselberger, "Canards in $\mathbb{R}^3$," J. Differ. Equations **177**(2), 419–453 (2001).

[32]F. Takens, "Constrained equations: a study of implicit differential equations and their discontinuous solutions," in *Structural Stability, the Theory of Catastrophes, and Applications in the Sciences*, Lecture Notes in Mathematics, Vol. 525 (Springer, 1976), pp. 143–234.

[33]D. Terman, "Chaotic spikes arising from a model of bursting in excitable membranes," SIAM J. Appl. Math. **51**(5), 1418–1450 (1991).

[34]K. Tsaneva-Atanasova, H. M. Osinga, T. Rieß, and A. Sherman, "Full system bifurcation analysis of endocrine bursting models," J. Theor. Biol. **264**(4), 1133–1146 (2010).

[35]These attracting branches stretch to infinity (while remaining strongly normally hyperbolic). This means that a typical technique of proving the existence of an invariant manifold (e.g., graph transform) can be applied without modifying the original vector field, by using test functions that stretch out to infinity. The slow manifolds obtained in this manner are analytic.